

Elevated ATPase Activity of KaiC Applies a Circadian Checkpoint on Cell Division in *Synechococcus elongatus*

Guogang Dong,^{1,2} Qiong Yang,³ Qiang Wang,⁵ Yong-Ick Kim,² Thammajun L. Wood,¹ Katherine W. Osteryoung,⁵ Alexander van Oudenaarden,^{3,4} and Susan S. Golden^{1,2,*}

¹Center for Biological Clocks Research, Department of Biology, Texas A&M University, College Station, TX 77843-3258, USA

²Center for Chronobiology, Division of Biological Sciences, University of California San Diego, 9500 Gilman Drive, La Jolla, CA 92093-0116, USA

³Department of Physics

⁴Department of Biology

Massachusetts Institute of Technology, Cambridge, MA 02139, USA

⁵Department of Plant Biology, Michigan State University, East Lansing, MI 48824, USA

*Correspondence: sgolden@ucsd.edu

DOI 10.1016/j.cell.2009.12.042

SUMMARY

A circadian clock coordinates physiology and behavior in diverse groups of living organisms. Another major cyclic cellular event, the cell cycle, is regulated by the circadian clock in the few cases where linkage of these cycles has been studied. In the cyanobacterium *Synechococcus elongatus*, the circadian clock gates cell division by an unknown mechanism. Using timelapse microscopy, we confirm the gating of cell division in the wild-type and demonstrate the regulation of cytokinesis by key clock components. Specifically, a state of the oscillator protein KaiC that is associated with elevated ATPase activity closes the gate by acting through a known clock output pathway to inhibit FtsZ ring formation at the division site. An activity that stimulates KaiC phosphorylation independently of the KaiA protein was also uncovered. We propose a model that separates the functions of KaiC ATPase and phosphorylation in cell division gating and other circadian behaviors.

INTRODUCTION

In organisms from microscopic cyanobacteria and fungi to plants and animals, genetically programmed daily cycles, known as circadian rhythms, pervade various aspects of physiology and behavior (Bell-Pedersen et al., 2005). In the cyanobacterium *Synechococcus elongatus*, the timing of cell division (Mori et al., 1996), global patterns of gene expression (Liu et al., 1995), and compaction of the chromosome (Smith and Williams, 2006) are all controlled by a circadian clock that exhibits the same properties as in eukaryotic organisms. However, the *S. elongatus* clock is distinct in components, mechanism, and

evolutionary history from eukaryotic clock systems (Dong and Golden, 2008; Mackey and Golden, 2007).

In *S. elongatus*, three neighboring genes, *kaiA*, *kaiB*, and *kaiC*, encode proteins of the central oscillator. Inactivation of any of them abolishes the clock, as does overexpression of KaiA or KaiC (Ishiura et al., 1998). KaiC is an autokinase, autophosphatase, and ATPase; in complex with KaiA and KaiB, KaiC displays a daily rhythm of phosphorylation at residues Ser431 and Thr432 (Nishiwaki et al., 2004; Xu et al., 2004) both in vivo and in vitro (Nakajima et al., 2005; Tomita et al., 2005). KaiA stimulates KaiC autophosphorylation and KaiB opposes KaiA's stimulatory activity (Iwasaki et al., 2002; Kim et al., 2008; Rust et al., 2007; Williams et al., 2002). The oscillation of KaiC phosphorylation in a mixture of the three Kai proteins and ATP in vitro (Nakajima et al., 2005) suggests that the phosphorylation cycle is the fundamental timekeeping mechanism in cyanobacteria. However, the ATPase activity of KaiC also oscillates in a circadian manner, is intrinsically temperature compensated, and determines circadian period length, suggestive of a timekeeping role that may be separable from the phosphorylation cycle (Terauchi et al., 2007). A gene expression rhythm persists in the absence of a KaiC phosphorylation rhythm (Kitayama et al., 2008); thus, other aspects of KaiC, such as the ATPase activity, may underlie the basic timing mechanism instead of, or in addition to, KaiC phosphorylation.

Temporal information from the cyanobacterial oscillator is broadcast to downstream genes via the histidine protein kinase SasA, whose autophosphorylation is stimulated by interaction with KaiC (Iwasaki et al., 2000; Smith and Williams, 2006). SasA then transfers the phosphoryl group to RpaA, a response regulator with a DNA-binding domain. Disruption of either *sasA* or *rpaA* results in severely damped rhythms or arrhythmia, depending on growth conditions (Iwasaki et al., 2000; Takai et al., 2006b).

An input pathway that includes CikA, LdpA, and Pex relays environmental information to the oscillator for synchronization (Dong and Golden, 2008). Both CikA and LdpA sense light indirectly through cofactors that perceive changes in the cellular

redox state, which varies with photosynthetic activity (Ivleva et al., 2005, 2006). CikA is found in a complex with LdpA, KaiA, KaiC, and SasA in vivo, but no direct biochemical interaction has been detected between CikA and the oscillator. A *cikA* null mutant exhibits short-period, low-amplitude gene expression rhythms and fails to reset the phases of rhythms after an environmental cue (Schmitz et al., 2000); additionally, it is defective in cell division, resulting in elongated cells (Miyagishima et al., 2005).

Cell division is a cyclic event that is tightly regulated by and coordinated with other cellular activities. Few studies to date have focused on the interaction between the cell and circadian cycles, with even fewer molecular details. For example, in regenerating liver cells of mice, circadian clock proteins directly control the expression of Wee1, a kinase that inhibits the entry into mitosis (Matsuo et al., 2003). Cell division is also gated by the clock in mouse fibroblast cells cultured in vitro (Nagoshi et al., 2004) and in *S. elongatus* (Mori et al., 1996). The rate of DNA synthesis is constant in the cyanobacterium and not phase dependent, suggestive of regulation further downstream—such as cytokinesis (Mori et al., 1996). The mechanism of cell division gating in *S. elongatus* has remained unknown in the face of rich molecular details of the cyanobacterial circadian clock. Elucidation of this pathway would tie the oscillator to a key fitness component of cell physiology.

Here, we show that elevated ATPase activity of KaiC closes the cell division gate and demonstrate a linear signal transduction pathway from the input components to the central oscillator and to the output pathway in the regulation of cell division. We also show that localization of the bacterial tubulin homolog FtsZ is a target of clock control. This work revealed the surprising action of a KaiA-independent, but CikA-suppressed, activity that stimulates KaiC autophosphorylation. A model of the relationship of KaiC ATPase and phosphorylation activities, and how they are incorporated with the input and output pathways of the clock, emerges from this work.

RESULTS

Cell Division Is Gated in the Wild-Type and *cikA* Mutant

A previous report showed the gating of cell division in a population of *S. elongatus* cells measured over several circadian cycles (Mori et al., 1996). That work predated the identification of molecular components of the cyanobacterial clock and did not address the process in individual cells. CikA is the only clock component that has been reported to play a role in cell division (Miyagishima et al., 2005); therefore, we tested the requirement of *cikA* for the gating of cell division. Using timelapse microscopy, we directly monitored growing cells for 3 days, recording events of cell division and the circadian rhythm of *kaiBC* promoter activity as reported by a destabilized yellow fluorescent protein, YFP-SsrA(LVA) (Chabot et al., 2007).

Individual mutant cells show rhythmic gene expression, with a period of 22.0 ± 1.1 hr, whereas the wild-type (WT) cells oscillate with a period of 24.9 ± 1.0 hr (Figure 1A), consistent with results from luciferase reporters (Schmitz et al., 2000). To address whether and how the circadian clock gates cell division, all division events were assigned to their corresponding cir-

cadian phases, normalized into one circadian period $0 \sim 2\pi$, and plotted as a histogram. To avoid sampling bias, we ensured that the initial circadian phases were evenly distributed; i.e., the cells examined are unsynchronized (data not shown). The occurrence of cell division in the WT is apparently suppressed around the peak of fluorescence (Figure 1B), indicating that cell division is gated. In the *cikA* mutant, a similar dip in the histogram was seen, although the overall occurrences of cell division during this window are higher and the duration of the inhibition is longer.

As a control we monitored cell division in an arrhythmic *kaiC* null mutant. Thus, the division events cannot be assigned to specific circadian phases. However, when we plotted the distribution of doubling time of all cells monitored (Figure 1C), the *kaiC* mutant had only a single peak in contrast to two peaks in the WT and *cikA* mutant. We reasoned that when gating is active, the doubling time of cells whose life spans cover the window of gating is prolonged compared to those whose life spans do not, resulting in two populations of cells with distinct doubling times. On the other hand, the doubling time of arrhythmic mutants follows a Gaussian distribution pattern in the absence of a gate. Both of these complementary types of analysis are able to detect gating of cell division. In conclusion, *cikA* is not essential to the gating of cell division, although its absence causes elongated cells and affects characteristics of the gate.

kaiC Is Epistatic to *cikA* in the Regulation of Cell Division

The phenotypic effects of a *cikA* null mutation on both circadian rhythms and cell length could be due to CikA's involvement in two pathways that separately govern circadian rhythms and cell division; alternatively, CikA may affect a clock pathway that regulates the gating of the cell cycle. If the second hypothesis is true, mutation of some clock genes would suppress the *cikA* null cell elongation phenotype. We made double mutants of *cikA* and central oscillator genes. Cell lengths of various mutants, grown under the same conditions simultaneously to minimize variations caused by cell density and/or light intensity (Figure S1 available online), were measured and compared. As expected, *cikA* mutant cells are significantly longer than the WT (Figures 1D and 1E). In the $\Delta kaiC \Delta cikA$ mutant, however, the absence of KaiC suppresses the cell division defect of *cikA*. The $\Delta kaiA \Delta cikA$ and $\Delta kaiB \Delta cikA$ mutants are still elongated. These data suggest that *cikA* regulates cell division through the clock, and that KaiC lies downstream of CikA in this pathway.

Loss of *kaiB* Leads to Increased Cell Length, Dependent on KaiC

To address the roles of other clock genes in cell-cycle control, single mutants were examined. Cells of a *kaiB* mutant average almost twice as long as WT, whereas mutants of *kaiA*, *kaiC*, or *ldpA* have normal cell lengths (Figures 1D and 1E and data not shown). The extensive evidence of KaiB-KaiC interaction suggested that inactivation of *kaiC* would also suppress the *kaiB* phenotype. Indeed, the cell length of a *kaiBC* double mutant is like WT (Figures 1D and 1E). We propose that the role of KaiB in determining cell length is the same as its function in modifying KaiC phosphorylation state.

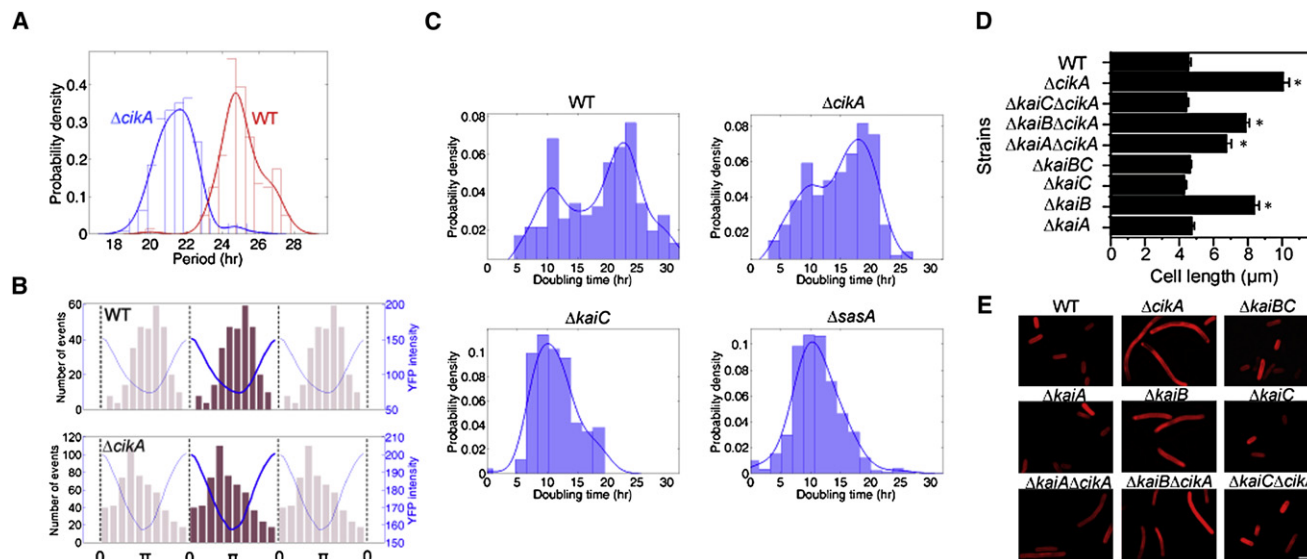


Figure 1. Gating of Cell Division and Comparison of Cell Lengths in Various Clock Mutants

(A) Distributions of circadian periods for WT (red) and *cikA* mutant (blue). Periods are defined as peak-to-peak time differences of individual cell traces. Curves are obtained by Gaussian kernel smooth with a kernel width of 0.5 hr.

(B) Histograms of phases for WT and *cikA* mutant. Phases are normalized to one period of $[0, 2\pi]$, where 0 starts at each YFP peak position. Averaged YFP signals (blue curves) were plotted on top of the histograms to indicate the gating position relative to *kaiBC* promoter activity. To highlight the periodicity of circadian cycles, data were copied (light pink) and shown adjacent to the original data (dark pink).

(C) Distributions of doubling time for the WT and three clock mutants. Doubling time of individual cells is defined as the time interval between two consecutive cell division events. Probability density is calculated by multiplying the bin width by the ratio of cell division events within one bin/all cell division events. Curves are obtained by Gaussian kernel smooth with a kernel width of 1.85 hr.

(D) Cell length of various clock mutants. An asterisk indicates that the cell length is significantly different from that of WT. $n > 150$. $p < 0.001$. Error bar = ± 1 standard error of the mean (SEM). Also see Figure S1.

(E) Representative micrographs of cells from (D). Autofluorescence from photosynthetic pigments distributed along the periphery of cells was captured. Scale bar = 5 μm . All subsequent figures use the same settings unless otherwise noted.

Constitutive Phosphorylation of KaiC Inhibits Cell Division

KaiB is known to inactivate KaiA to initiate KaiC dephosphorylation (Rust et al., 2007). Loss of *kaiB* abolishes circadian rhythms (Ishiura et al., 1998) and results in constitutively phosphorylated KaiC both in vivo (Figure 2C) and in vitro (Iwasaki et al., 2002; Kitayama et al., 2003). CikA also affects KaiC phosphorylation state (Ileva et al., 2006). Therefore, we asked whether constitutively phosphorylated KaiC is the cause of cell division inhibition. To stimulate KaiC phosphorylation, we overexpressed KaiA from an IPTG (isopropyl- β -D-thiogalactopyranoside)-inducible *trc* promoter in a WT background, which abolishes circadian rhythms of gene expression and KaiC phosphorylation (Ishiura et al., 1998; Kitayama et al., 2008), and in a *kaiC* null background in parallel. Cells overexpressing KaiA in the presence of KaiC are significantly longer than those in the *kaiC* null background and in WT cells after IPTG addition, whereas no difference was observed before induction (Figures 2A and 2B). Note that, during the 5 day induction period, WT cells also lengthened, which is due to higher cell density and/or lower light penetration and not related to IPTG (Figure S1). Interestingly, the *cikA* mutant's cell length is much more affected by culture density than the WT (Figure S1A). We confirmed that KaiC becomes and stays highly phosphorylated after IPTG induction (Figure 2C and data not shown). We further demonstrated that the cell elongation

phenotype is reversible by removing IPTG after days of KaiA-YFP overexpression (Figure S2).

Recently, several KaiC variants were created that are constitutively hyper- or hypophosphorylated independent of KaiA or KaiB (Kim et al., 2008). KaiC487, a truncation mutant missing the last 32 aa, and the missense mutant KaiCE444D are both highly phosphorylated, whereas KaiC497 remains unphosphorylated. We expressed these alleles in a *kaiC* null mutant and, consistent with the hypothesis that phosphorylated KaiC is an inhibitor of cell division, both KaiC487 and KaiCE444D caused cell elongation whereas KaiC497 did not (Figures 2D and 2E).

KaiC Can Be Phosphorylated Independently of KaiA In Vivo

Cells of the $\Delta k ai A \Delta c i k A$ mutant are elongated (Figures 1D and 1E), which was intriguing because all evidence had suggested that phosphorylated KaiC inhibits cell division, yet KaiA is required for KaiC phosphorylation. We examined the KaiC phosphorylation state in this strain and found it $\sim 60\%$ phosphorylated, in contrast to being fully unphosphorylated in the $\Delta k ai A$ strain (Figure 2C). No oscillation in gene expression or KaiC phosphorylation is observed in the $\Delta k ai A \Delta c i k A$ mutant (Figure S2). We concluded that an unknown activity is able to stimulate KaiC phosphorylation independently of KaiA, and that this cryptic activity is inhibited by CikA. Furthermore, KaiC

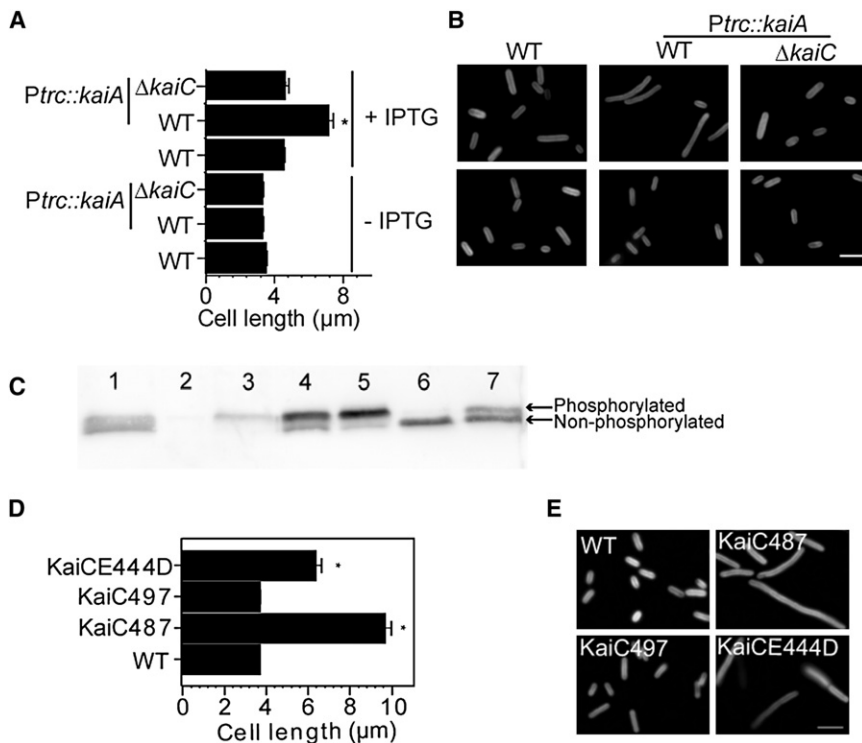


Figure 2. Constitutive Phosphorylation of KaiC Inhibits Cell Division

(A) KaiA overexpression causes cell elongation in the WT background but not in a *kaiC* null background. Error bar = ± 1 SEM. See also Figure S2. (B) Representative micrographs of cells from (A). (C) Immunoblots of various strains showing KaiC phosphorylation states. Lane 1: WT; 2: Δ *kaiC*; 3: Δ *kaiB*; 4 and 5: *Pptrc::kaiA* expressed in the WT background in the absence (4) or presence (5) of 1 mM IPTG; 6: Δ *kaiA*; 7: Δ *kaiA* Δ *cikA*. See also Figure S2. (D) KaiC487 and KaiCE444D mutants cause cell elongation whereas KaiC497 does not. Error bar = ± 1 SEM. (E) Representative micrographs of cells from (D).

still inhibits cell division suggests that KaiC phosphorylation is not required for cell elongation.

Elevated ATPase Activity of KaiC Correlates with Elongated Cells

The underlying signal that inhibits cell division must be a state or activity of KaiC that is usually coupled with, but functionally separable from, phosphorylation. Aside from autokinase and autophosphatase

activities, KaiC has an unusually low ATPase activity that fits this description (Terauchi et al., 2007). Two Walker's A motifs are located at the N and C termini of KaiC (Figure 4A). The N-terminal motif is important in the hexamerization of the protein and the C-terminal motif is essential for autophosphorylation (Hayashi et al., 2004, 2006). KaiC hydrolyzes ATP in a circadian manner, and phosphorylation of KaiC accounts for only a negligible portion of the total ATP consumed per cycle.

Phosphorylation of KaiC Is Not Essential for Cell Elongation

The underlying signal that inhibits cell division must be a state or activity of KaiC that is usually coupled with, but functionally separable from, phosphorylation. Aside from autokinase and autophosphatase activities, KaiC has an unusually low ATPase activity that fits this description (Terauchi et al., 2007). Two Walker's A motifs are located at the N and C termini of KaiC (Figure 4A). The N-terminal motif is important in the hexamerization of the protein and the C-terminal motif is essential for autophosphorylation (Hayashi et al., 2004, 2006). KaiC hydrolyzes ATP in a circadian manner, and phosphorylation of KaiC accounts for only a negligible portion of the total ATP consumed per cycle.

KaiC phosphorylation is a dynamic process and four forms of KaiC cycle in a stepwise fashion (Figure 3A) (Nishiwaki et al., 2007; Rust et al., 2007). By replacing S431 and T432 with Glu, Asp, or Ala, Nishiwaki et al. (2007) mimicked different phosphoforms of KaiC and characterized certain properties of the Kai oscillator in vitro. We hypothesized that the KaiCS431D, T432E (KaiC-DE) mutant, which mimics fully phosphorylated KaiC, would inhibit cell division whereas KaiC-AA, mimicking unphosphorylated KaiC, would have no effect. We made other phosphomimetics to further dissect the relationship between KaiC phosphorylation and cell division. The results, however, were opposite to our predictions: the strain expressing KaiC-DE has WT cell length, but those expressing either KaiC-AA or KaiC-AE show inhibition of cell division (Figures 3B and 3C). All variants except KaiC-SE were expressed at levels comparable to those in WT (Figure 3D), ruling out the possibility that KaiC-DE abundance is insufficient to inhibit cell division; KaiC-SE was undetectable and thus uninformative (data not shown). We have clearly shown that phosphorylated KaiC or a specific activity coupled with it causes cell elongation, whereas unphosphorylated native KaiC has no effect. Therefore, these KaiC phosphomimetics are not completely faithful representations of the different KaiC phosphoforms. The fact that KaiC-AA cannot be phosphorylated, does not mimic phosphorylated KaiC, and yet

activities, KaiC has an unusually low ATPase activity that fits this description (Terauchi et al., 2007). Two Walker's A motifs are located at the N and C termini of KaiC (Figure 4A). The N-terminal motif is important in the hexamerization of the protein and the C-terminal motif is essential for autophosphorylation (Hayashi et al., 2004, 2006). KaiC hydrolyzes ATP in a circadian manner, and phosphorylation of KaiC accounts for only a negligible portion of the total ATP consumed per cycle.

About 15 ATP molecules are consumed per KaiC monomer per day when incubated alone (hereafter, 1 unit = 1 ATP \times monomer⁻¹ \times day⁻¹); this number increases about 2-fold in the presence of KaiA. The KaiC-AA mutant has a constitutively high ATPase activity of ~ 27 units, whereas KaiC-DE hydrolyzes ~ 11 units (Terauchi et al., 2007). Thus, we hypothesized that elevated ATPase activity, rather than phosphorylation of KaiC, triggers inhibition of cell division. To test this hypothesis, we made four ATPase mutant variants of KaiC-AA based on previous reports (Hayashi et al., 2003, 2004; Nishiwaki et al., 2000) and expressed them in a *kaiC* null strain. KaiC^{K52H}-AA and KaiC^{catE1}-AA are expected to inactivate ATPase activity in the N-terminal domain and KaiC^{K294H}-AA and KaiC^{catE2}-AA to inactivate activity in the C-terminal domain. All ATPase mutants have reduced cell length compared to KaiC-AA, but three out of the four (KaiC^{catE1}-AA, KaiC^{K294H}-AA, and KaiC^{catE2}-AA) mutants are still elongated compared to the WT (Figure 4C). We then attempted to express a variant in which the catalytic Glu residues from both domains are replaced (KaiC^{catE1catE2}-AA). Although this mutant has WT cell length, immunoblot analysis showed that it is not detectable, nor is KaiC^{K52H}-AA, whereas the other three mutants are expressed at levels comparable to KaiC-AA (Figure 4B).

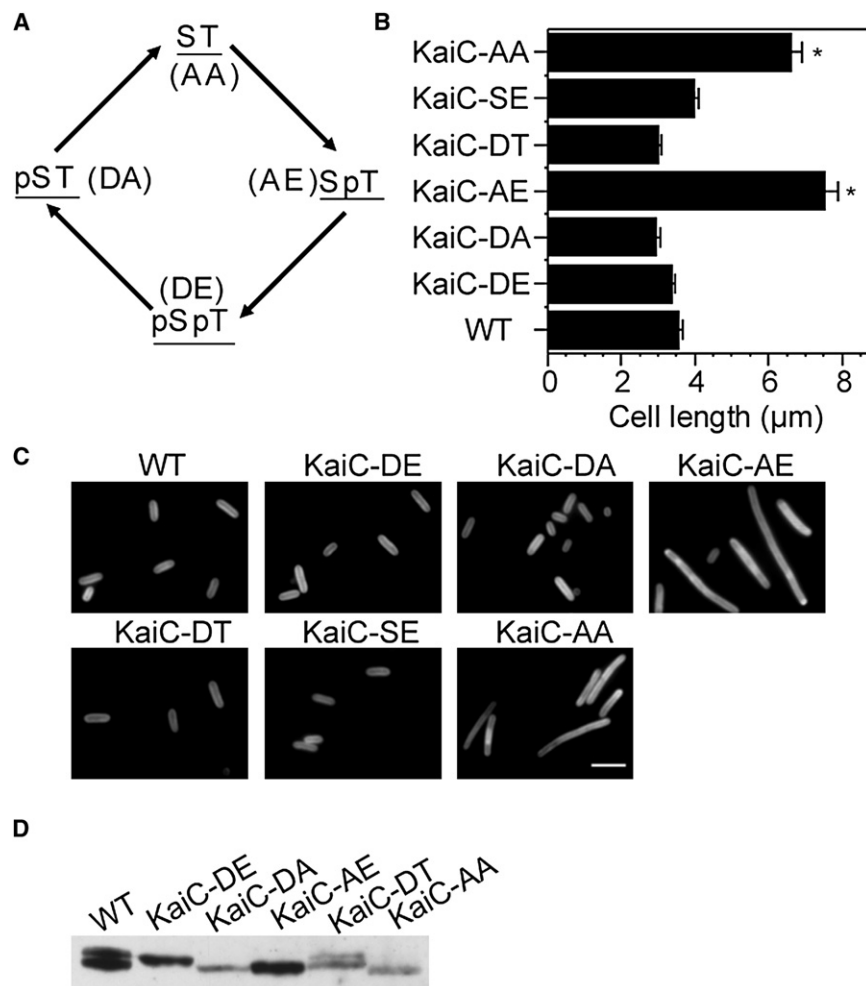


Figure 3. Constitutive KaiC Phosphorylation Is Not Required for Cell Elongation

(A) Ordered phosphorylation steps of KaiC and amino acid substitutions that mimic each phosphoform.

(B) Effects of KaiC phosphomimetics on cell length. Error bar = ± 1 SEM.

(C) Representative micrographs of cells shown in (B).

(D) Immunoblot of KaiC demonstrates the expression of KaiC phosphomimetics. KaiC-SE was undetectable and thus not shown.

assay) in the presence of both KaiA and KaiB; values for KaiA and KaiB alone were negligible (0.4 units). In contrast, KaiC^{catE2}-AA activity is not altered, and KaiC^{catE1}-AA activity is stimulated only 2-fold, when mixed with the other Kai proteins (Figures 4E and 4F); both values are lower than for KaiC-AA but higher than the WT, which could explain the elongated cell phenotype seen in these two mutants. KaiC-AA and KaiC-AE do not interact with KaiB but do with KaiA (Nishiwaki et al., 2007); thus, we speculate that even when both KaiA and KaiB are present, KaiC-AA and KaiC-AE would likely interact only with KaiA and have their ATPase activities elevated.

To further test our hypothesis, we compared cell lengths among different KaiC period mutants because KaiC mutants with higher ATPase activities

We then purified recombinant KaiC mutant proteins and measured their ATP hydrolysis activity in vitro by using C18 reversed-phase high-performance liquid chromatography (HPLC) to separate and quantify ADP from ATP. We predicted that mutations causing cell elongation would also elevate ATPase activities. We chose KaiC487, KaiC497, KaiC-AE, KaiC^{catE1}-AA, and KaiC^{catE2}-AA because their values have not been reported and included WT KaiC, KaiC-DE, and KaiC-AA as controls. Consistently, KaiC (12.6 ± 1.1), KaiC-DE (16.7 ± 0.8), and KaiC-AA (27.1 ± 1.1) values were comparable to published data (Figure 4E and Terauchi et al., 2007). KaiC487 hydrolyzes 59.6 ± 4.1 ATP units, 4- to 5-fold higher than the WT, whereas KaiC497 hydrolyzes 14.3 ± 0.3 units. Surprisingly, values from KaiC^{catE1}-AA and KaiC^{catE2}-AA were higher than that of KaiC-AA (Figure 4E), and KaiC-AE's ATPase activity is the same as WT. Because these data were not consistent with our hypothesis, we tested whether adding KaiA and KaiB to the in vitro system at appropriate ratios to mimic more closely the in vivo system would alter the ATPase activities, recognizing that we had expressed these mutants in a *kaiC* null background where both KaiA and KaiB were present. Indeed, KaiC-AE and KaiC-AA hydrolyze at least 330 units (which is saturation of the

exhibit shorter periods, whereas those with lower activity have longer periods (Terauchi et al., 2007). We picked two KaiC mutants whose ATPase activities have been quantified—KaiCR393C with a 15 hr period and KaiCA251V with a 46 hr period—as well as two other KaiC period mutants—KaiCR321Q (22 hr) and KaiCT409A (27 hr)—to compare their cell lengths. As predicted, KaiCR393C mutant cells were longer than the KaiCR321Q mutant, and both were longer than the WT and long period mutants, which were not different from each other (Figure 4D).

Elevated ATPase activity could be achieved by an increase in either the enzymatic activity of individual KaiC molecules or the abundance of the enzyme. Our results demonstrated inhibition of cell division by elevated intrinsic ATPase activity; therefore, we tested whether an increase of total ATPase activity has a similar effect. We overexpressed WT KaiC in a *kaiC* null background, confirmed abundance by immunoblot (data not shown), and monitored cell length. No difference was seen between cells that overexpress KaiC and those that do not (Figure S3), indicating that the intrinsic ATPase activity of KaiC, rather than the total amount of ATP hydrolyzed, signals inhibition of cell division. This result is in line with the remarkably low ATPase activity

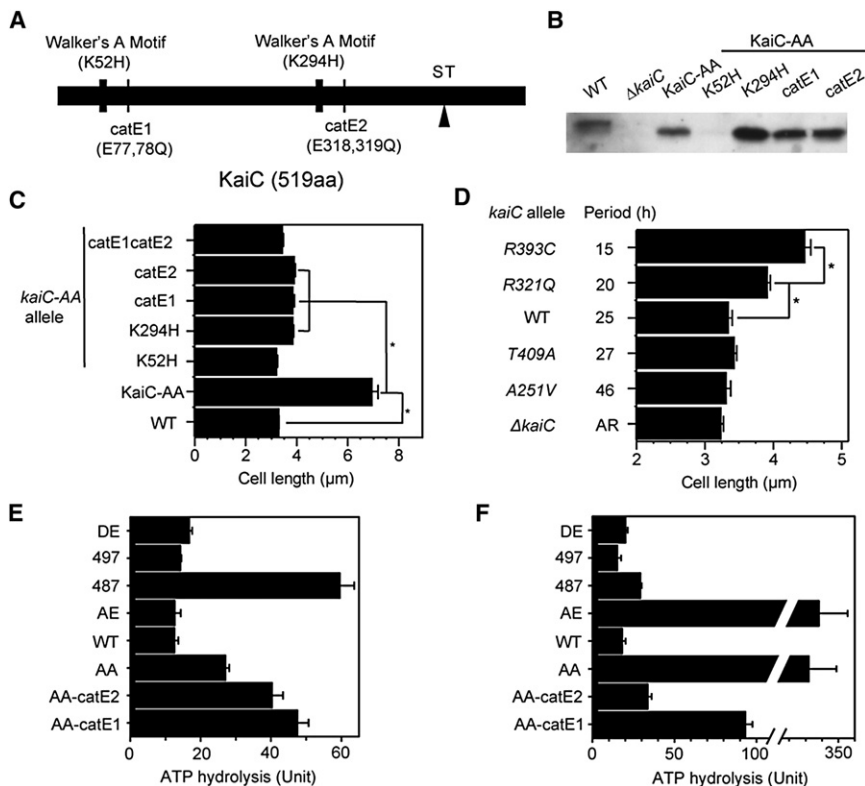


Figure 4. High ATPase Activity of KaiC Coincides with Cell Elongation

(A) Illustration of Walker's A motifs identified in KaiC and point mutations used to disrupt them.

(B) Immunoblot of KaiC reveals the expression level of KaiC ATPase mutants.

(C) Point mutations that disrupt ATPase motifs significantly reduce cell length in the KaiC-AA mutant. Error bar = ± 1 SEM.

(D) Circadian period and cell length. An asterisk marks statistically significant difference of cell lengths between the connected strains. Error bar = ± 1 SEM.

(E) ATPase activity of KaiC WT and mutant variants expressed in units of 1 ATP hydrolyzed \times KaiC monomer $^{-1} \times$ day $^{-1}$. Error bar = ± 1 SEM.

(F) ATPase activity of KaiC WT and mutant variants incubated with KaiA and KaiB, reported as in (E). Error bar = ± 1 SEM.

See also Figure S3.

exhibited by KaiC, making it unlikely to affect the cellular ATP pool if the measured values hold true in vivo.

The SasA-RpaA Output Pathway Is Epistatic to Cika and KaiC in the Control of Cell Division

Mutants of the clock output pathway genes *sasA* or *rpaA* do not have cell elongation phenotypes (Figures 5A and 5B and data not shown). To test whether this output pathway governs the circadian gating of cell division, cell lengths of double mutants of *cika* with *sasA* (Δ *cika* Δ *sasA*) and *kaiB* with *sasA* (Δ *kaiB* Δ *sasA*) or *rpaA* (Δ *kaiB* Δ *rpaA*) were compared to the WT and single mutants. In all cases, mutation of *sasA* or *rpaA* restored cells to WT length (Figures 5A and 5B). Because *kaiBC* expression is significantly reduced in the *sasA* mutant (Iwasaki et al., 2000), it was possible that the suppression phenotype in the double mutants was merely a result of a reduction in KaiC abundance. Therefore, we introduced a copy of WT *kaiC* expressed from the *trc* promoter into the Δ *kaiB* Δ *sasA* background and elevated KaiC expression by adjusting the concentration of IPTG. Cells maintained WT length regardless of KaiC abundance (Figures 5C and 5D), suggesting that SasA-RpaA is indeed downstream of KaiC in the control of cell division. Thus, we hypothesized that gating of cell division would be abolished in the *sasA* mutant. Using the same YFP-LVA reporter from Figure 1, we examined cell division in the *sasA* mutant using timelapse microscopy and did not detect rhythmic gene expression. Nonetheless, the distribution of doubling time showed a single peak (Figure 1C), indicating that no gating of cell division is present when the clock output is disrupted.

although FtsZ abundance is unaffected (Miyagishima et al., 2005). Targeting FtsZ to regulate cell division is a common theme in bacteria (Kawai et al., 2003; Weart et al., 2007). If the circadian clock blocks FtsZ localization at the division site, an increase in the FtsZ level might overwhelm the inhibition and allow cell division. Thus, we expressed *ftsZ* from *trc* in the *cika*, *kaiB*, and *kaiC-AA* mutant backgrounds. In all cases, cell length was significantly reduced even in the absence of IPTG (Figure 6A), suggesting that an elevated level of FtsZ suppresses the cell division defect caused by the clock mutants. Immunoblots confirmed that the level of FtsZ was the same between the WT and elongated mutants but was elevated about 2-fold in the suppressor mutants that have ectopic *ftsZ* expression (Figure 6B).

We then examined FtsZ localization in these strains by immunofluorescence microscopy (Figure 6A). FtsZ was frequently mislocalized in the elongated mutants and was often concentrated at the cell poles or observed in patches, with some rings localized away from midcell along the elongated cells. In contrast, *ftsZ*-compensated mutants have a higher frequency of correctly localized FtsZ rings. Therefore, we conclude that FtsZ ring localization and assembly are events that are targeted by the circadian clock machinery in the regulation of the timing of cell division.

DISCUSSION

ATPase Activity of KaiC Provides a Checkpoint on Cell Division

The circadian clock imposes a checkpoint on cell division by actively inhibiting cytokinesis at specific circadian times; the

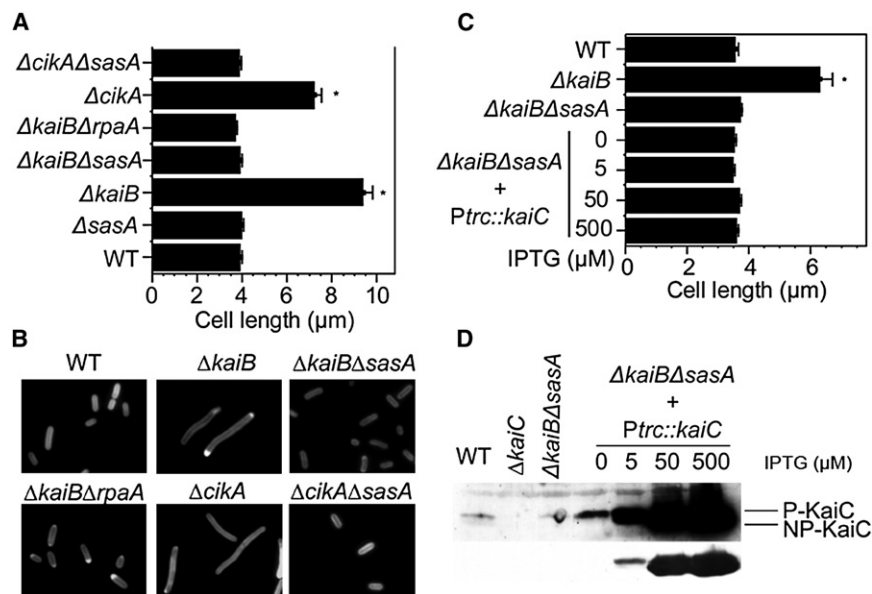


Figure 5. SasA and RpaA Are Downstream of CikA and the Central Oscillator in the Control of Cell Division

(A) Knockout of *sasA* or *rpaA* from *cikA* or *kaiB* null strains releases inhibition of cell division. Error bar = ± 1 SEM.

(B) Representative micrographs of cells from (A). (C) Elevated level of KaiC does not induce the cell elongation phenotype in the $\Delta kaiB \Delta sasA$ strain. Error bar = ± 1 SEM.

(D) Immunoblot analysis shows abundance of KaiC in strains measured in (C). The lower panel is a shorter exposure of the upper panel. KaiC is less abundant in the $\Delta kaiB \Delta sasA$ strain than in WT; expression of *Ptrc::kaiC* in this background elevated KaiC level to different degrees, depending on the concentration of IPTG. Even at 0–5 μ M IPTG, KaiC is higher than in the WT and is predominantly in the phosphorylated form.

absence of a clock does not affect cell division. By default the gate is open so that cell division operates independently of the clock and closes as ATPase activity of KaiC rises above a threshold value (Figure 6C). The signal is transmitted through SasA-RpaA to inhibit midcell FtsZ ring assembly, blocking cytokinesis of cell division until ATPase activity falls below the threshold (Figure 6D). With a functional clock, KaiC variants with higher ATPase activities would spend more time per day above the threshold, resulting in longer cells. In arrhythmic mutants where KaiC is locked in a high ATPase state, the gate is constitutively closed and cells should elongate infinitely. However, a bypass pathway seems to enable cell division, albeit at a much lower frequency, which explains the nonlethal phenotype in these mutants. The cryptic bypass pathway and disruption of interactions with non-Kai cellular partners may contribute to the lack of direct correlation between cell length and the ATPase activity measured in vitro among the arrhythmic mutants (KaiC487, KaiC-AA, KaiC-AE, etc.), as other unknown factors affect cell length. For example, cell density affects $\Delta cikA$ cell length more dramatically than that of WT (Figure S1). KaiA overexpression under the microscopic monitoring conditions caused cells to grow without dividing for about 3 days and reach 40 μ m (Figure S2), but in liquid culture the same genotype maintains an average cell length of ~ 7 μ m (Figure 2). The structurally locked, or even truncated variants (KaiC487) may be differentially defective in unknown partner interactions.

Peak KaiC ATPase activity occurs 4 hr before that of phosphorylation in vitro (Terauchi et al., 2007), whereas the in vivo phosphorylation peak is ~ 16 hr after light onset (CT 16) (Tomita et al., 2005); we estimate that KaiC ATPase activity peaks around CT 12 in vivo (Figure 6C). The center of the gate occurs around the peak of YFP fluorescence, which is around CT 17 (data not shown). Therefore, there is a delay between KaiC ATPase and gating of cell division, which may represent multiple steps of signal transduction (Figure 6D).

A Model of the Circadian Clock in *S. elongatus*

We propose that KaiC ATPase and phosphorylation are closely coupled but functionally distinct: stepwise KaiC phosphorylation and dephosphorylation (Nishiwaki et al., 2007; Rust et al., 2007) govern the interaction dynamics among the Kai proteins to form a core oscillator, whereas ATPase activity connects the oscillator with the input and output pathways to drive circadian behaviors. Specifically, elevated KaiC ATPase activity stimulates the SasA output pathway, and KaiB competes with SasA for KaiC binding and lowers KaiC ATPase activity (Iwasaki et al., 2000; Terauchi et al., 2007) to turn down the output (Figure 6D).

We propose that a specific KaiC conformational state associated with elevated ATPase activity stimulates SasA autophosphorylation and triggers the inhibition of cytokinesis; this hypothesis is consistent with KaiC's identity in the RecA/DnaB superfamily, whose members couple ATP hydrolysis with conformational changes (Wang, 2004; Ye et al., 2004). Because some KaiC mutants hydrolyze >10 times more ATP than reported previously in the presence of KaiA and KaiB (Figure 4F), it cannot be ruled out that KaiC possesses much higher ATPase activity in vivo when specific conformational states interact with other partners we have not tested in vitro.

The data are consistent with a model in which elevated ATPase activity turns on the SasA-RpaA gene expression regulatory pathway as well, whereas lower ATPase activity shuts it off, which feeds back on the transcription of *kaiBC*. This loop, with appropriate levels of positive (high ATPase activity of KaiC) and negative elements (such as proteases), could potentially generate an autonomous rhythm in the absence of a KaiC phosphorylation rhythm, which has been reported (Kitayama et al., 2008).

How Is CikA Involved?

Until this work, it was unclear whether the *cikA* mutant's circadian rhythm and cell division phenotypes are related. We show

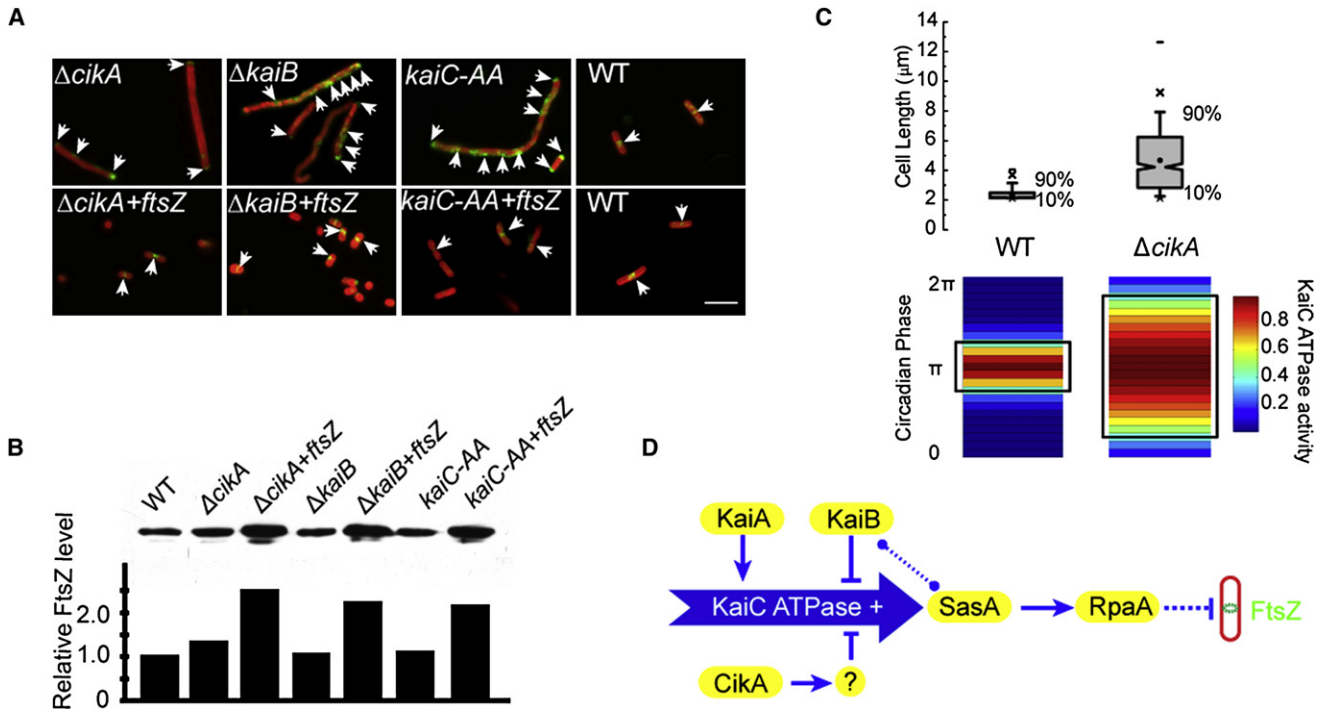


Figure 6. Localization of FtsZ Is Regulated by the Circadian Clock

(A) Suppression of mislocalized FtsZ in elongated cell clock mutants by ectopic expression of *ftsZ*. FtsZ was detected by immunofluorescence microscopy. Red indicates autofluorescence from phycobilisomes, whereas green is the FtsZ signal. White arrows indicate FtsZ localization.

(B) Comparison of FtsZ levels in the WT and strains measured in (A). Top: immunoblot using FtsZ antiserum. Bottom: quantification of the relative levels of FtsZ shown on top. Level of FtsZ in the WT is set at 1.

(C) A model of gating of cell division by elevated ATPase activity of KaiC. The bottom panel is the ATPase activity of KaiC for WT and the $\Delta cikA$ mutant in one circadian period represented in colormaps, with the maximum activity normalized to 1. When ATPase activity is above a certain threshold as indicated in the black frames overlaying the colormaps, cell division is inhibited; this inhibition window is termed the “gate.” In the $\Delta cikA$ mutant, ATPase activity still oscillates, but the basal level is elevated due to the stimulation from an unknown factor, which results in a wider window of inhibition of cell division every day, and thus the larger cell size. The box plots in the top panel depict cell length distributions, which depend on the different inhibition windows of WT and the $\Delta cikA$ mutant. Cell lengths are generated by stochastic simulation based on a gating model described in Figure S4.

(D) A signal transduction pathway of the circadian clock in gating cell division. KaiA stimulates KaiC ATPase activity, and KaiB lowers it. CikA represses KaiC ATPase activity through an unknown activity (question mark). Elevated ATPase activity of KaiC (+) activates SasA and subsequently RpaA, turning on the output pathway, which in turn disturbs FtsZ localization at the septation site (likely to be indirect). KaiB may compete with SasA (dotted line with knobs) while lowering KaiC ATPase activity to turn down the output pathway.

that all known *cikA* phenotypes are a function of the circadian clock. We propose that in a *cikA* null, KaiC ATPase activity still oscillates but at a higher level, which would result in a wider window of cell division gating and longer cells (Figure 6C). Most significantly, the model predicts that CikA resets the clock by modulating ATPase activity of KaiC. During a dark pulse, CikA abundance goes up (Ileva et al., 2006), which in turn would suppress the ATPase activity of KaiC. At the same time abundance of Pex, a transcriptional repressor of *kaiA*, also goes up (Kutsuna et al., 2007; Takai et al., 2006a), decreasing KaiA expression and reducing stimulation of KaiC ATPase activity. We suggest that these events work synergistically to achieve a delay in KaiC phosphorylation or an advance in KaiC dephosphorylation, with the CikA-modulated pathway playing a dominant role in resetting.

The discovery of a KaiA-independent, but CikA-repressed, factor that stimulates KaiC ATPase activity suggests that there

are at least two pathways that regulate KaiC ATPase activity *in vivo*: a KaiA-KaiB-KaiC loop and a CikA-mediated pathway that converge on KaiC and enhance the robustness of the circadian clock. Consequently, the CikA-dependent pathway is also a part of the regulatory mechanism for gene expression rhythms. In CikA's absence, KaiA and KaiB, the main drivers of the oscillation of KaiC's ATPase activity, continue to support rhythmic gene expression, but the period is shortened and amplitude reduced. Overexpression of CikA completely abolishes circadian rhythms of gene expression (Zhang et al., 2006). Both of these phenotypes may stem from the previously unknown KaiC-stimulating pathway. This CikA-mediated pathway may also contribute to the gene expression rhythm that is observed in the absence of a KaiC phosphorylation rhythm (Kitayama et al., 2008). We predict that eliminating CikA from these strains would at least weaken, if not abolish, the residual rhythms.

SasA- and RpaA-Mediated KaiC-Dependent Gating of Cell Division

We identified FtsZ as a target of the SasA-RpaA-mediated circadian checkpoint. It has been reported that promoter activity of *ftsZ* is rhythmic (Mori and Johnson, 2001) and suggested that circadian oscillation of FtsZ level underlies gating of cell division (Mori, 2009). However, our results indicate that polymerization or localization of FtsZ is regulated rather than its abundance. Because FtsZ plays a vital role in cell division in bacteria, we speculate that such a dedicated pathway can exert precise effects from the clock at a specific time without tying the rate of cell division to the clock at all times.

Because RpaA is predicted to be a transcription factor, and it participates in posttranslational regulation of FtsZ, intermediate steps of signal transduction likely exist. Other potential targets of clock control include components of the Min system and/or a homolog of DivIVA. Although these proteins have been scarcely studied in cyanobacteria (Mazouni et al., 2004; Miyagishima et al., 2005), related proteins in other bacteria regulate the position and timing of FtsZ ring assembly (Gregory et al., 2008; Lutkenhaus, 2007; Margolin, 2005).

Why Does the Circadian Clock Gate Cell Division?

The biological significance of cell division gating by the circadian clock remains unknown. Perhaps a closed gate protects the clock from asymmetric distribution of components at some points in the circadian cycle, such as during monomer shuffling. The *S. elongatus* clock is inherited with exceptional fidelity (Mihalcescu et al., 2004), and it stands to reason that a checkpoint exists to safeguard this accuracy. Alternatively, the gate protects other cellular events from damage that might result from cytokinesis at a vulnerable time, such as when the chromosome is in a particular compaction state (Smith and Williams, 2006). However, the nucleoid occlusion effect, which is seen in many other bacteria, is absent in *S. elongatus*, as FtsZ ring formation can occur over chromosomal DNA (Miyagishima et al., 2005). The gate coincides with the onset of darkness, when oxidative stress and UV damage would be lower than during daytime. Cell division is restricted to the reductive phase of the metabolic cycle in yeast under nutrient-limiting conditions, probably to protect genome integrity (Chen et al., 2007). However, *S. elongatus* does not restrict its cell division to the dark, and the rate of DNA replication, the process most sensitive to UV damage or oxidative stress, remains constant during the circadian cycle (Mori et al., 1996); cytokinesis, rather than replication, is targeted. Overall, the data suggest that gating of cell division in *S. elongatus* does not exist to protect the genome from damage caused by stress conditions. With limited information, we favor the hypothesis that gating protects the accuracy of the clock.

In summary, we provide mechanistic insights into the gating of cell division and the circadian clock. Moreover, this study shows an unprecedented linear flow of information from known components of the input (CikA), oscillator (KaiC), and output (SasA/RpaA) divisions of the clock (Figure 6D). Further study not only will deepen our knowledge of the circadian clock but also will uncover the intricate interactions of two major cellular oscillators with global physiological impact that cycle with different periods.

EXPERIMENTAL PROCEDURES

Bacterial Cultures, Growth Conditions, and DNA Manipulations

S. elongatus PCC 7942 and its genetic variants were propagated as previously described (Clerico et al., 2007; Mackey et al., 2007), except that when multiple antibiotics were needed, concentrations of gentamycin and kanamycin were halved. Mutant alleles were made using the QuickChange (Stratagene, La Jolla, CA, USA) protocol and clones were verified by DNA sequencing. A list of plasmids, propagated in *E. coli* DH10B, and cyanobacterial strains used in this study is detailed in Tables S1 and S2.

Sample Preparation and Epifluorescence Microscopy

Strains were grown in liquid medium in a shaking incubator at a light intensity of $45 \mu\text{E m}^{-2} \text{s}^{-1}$. The following routine minimized variations in cell length due to light intensity, growth phase, etc.: 5 ml of liquid culture was subcultured into 100 ml fresh BG-11 medium with appropriate antibiotics, grown for 3 days, and subcultured into 100 ml medium with a 1:100 dilution factor. Cell length was measured for all strains at the same time after 3–4 days of growth. Cells collected from 1 ml culture were resuspended in 100 μl sterile water; 2 μl samples were loaded on a glass slide, followed by 5 μl of 1% low-melting agarose dissolved in BG-11 medium, and were covered with a cover glass. Autofluorescence images were taken using an Olympus Ix 70 inverted microscope with a 100 \times oil-immersion objective.

Image Processing and Statistical Analysis

Micrographs of cyanobacterial cells were saved as 8-bit gray images. Analysis was performed with ImageJ (<http://rsbweb.nih.gov/ij/>). Cells that were touching were manually separated by a 5 pt black line or were excluded from analysis. Images were segmented using the "Otsu Thresholding 8bit" plugin and cell length was acquired by applying the "Measure Roi Curve" plugin function, with default settings, to the segmented images. Data were imported into SPSS 14.0 and compared using Dunnett's T3 algorithm in One-way ANOVA analysis with $p < 0.001$.

Timelapse Microscopy

Timelapse microscopy experiments were performed on strains that were grown under the standard conditions at a light intensity of $25 \mu\text{E m}^{-2} \text{s}^{-1}$. Cultures were diluted 3 days before acquisition so that their optical densities (OD)₇₅₀ were <0.2 . For each sample, 1.5 μl of cells were loaded in one of two wells of a glass chamber (LAB-TEK) and covered with a square pad of 2% low-melting agarose. Next, a liquid 2% low-melting agarose was poured on top of the first solid pad and the chamber was loaded on the microscope for imaging. Phase contrast and YFP images were taken every 40 min for a total of 16 positions for each sample. The acquisition period typically lasted 3 days, during which a constant cool-white fluorescent light source illuminated the sample with an intensity of $30 \sim 50 \mu\text{E m}^{-2} \text{s}^{-1}$ except during image acquisition. The images were analyzed with custom-written MATLAB software to track each single cell as it divided and oscillated.

Immunofluorescence Microscopy and Immunoblots

Immunofluorescence microscopy on FtsZ was performed as previously described (Miyagishima et al., 2005). Immunoblots were performed as described (Ileva et al., 2005), except that KaiC antiserum was used at 1:2000 dilution.

ATPase Assay

KaiA, KaiB, KaiC, and KaiC mutant proteins were expressed in *E. coli* BL21DE3 and purified as described (Iwasaki et al., 2002; Kim et al., 2008; Rust et al., 2007; Williams et al., 2002). ATPase assays of KaiC and its variants (3.5 μM) were performed in sterile 1.5 ml tubes with or without KaiA and KaiB (1.2 and 3.5 μM , respectively) in the standard buffer (150 mM NaCl, 20 mM Tris-HCl, 5 mM MgCl₂, 0.5 mM EDTA, 1.3 mM ATP, and pH = 8.0). To separate ATP and ADP in the reaction mixture, chromatography was carried out on a Vydac C18 column with 250 mM phosphate buffer (pH 5.0) as a mobile phase. The amount of ADP produced in the reaction mixture was calculated from the area of the ADP peak. Values were calculated from two assays for WT and from three assays for all variants.

SUPPLEMENTAL INFORMATION

Supplemental Information includes four figures and two tables and can be found with this article online at doi:10.1016/j.cell.2009.12.042.

ACKNOWLEDGMENTS

We thank P. Luitel for helpful discussions, A. LiWang for sharing instrumentation and unpublished data, C.-C. Zhang for providing the FtsZ antiserum, and A. Suescun for technical assistance. We are grateful to J. Xiao, T. Liu, and I. M. Axmann for constructive suggestions on the ATPase assays. This work was supported by grants from the NIH (R01 GM62419 and P01 NS39546 to S.S.G., R01 GM068957 to A.v.O.), the American Recovery and Reinvestment Act (S.S.G.), NSF (PHY-0548484 to A.v.O.), and DOE (DE-FG-02-06ER15808 to K.W.O.). The content is solely the responsibility of the authors and does not necessarily represent the official views of the National Institute of General Medical Sciences or the National Institutes of Health.

Received: May 23, 2009

Revised: October 13, 2009

Accepted: December 21, 2009

Published: February 18, 2010

REFERENCES

- Bell-Pedersen, D., Cassone, V.M., Earnest, D.J., Golden, S.S., Hardin, P.E., Thomas, T.L., and Zoran, M.J. (2005). Circadian rhythms from multiple oscillators: lessons from diverse organisms. *Nat. Rev. Genet.* **6**, 544–556.
- Chabot, J.R., Pedraza, J.M., Luitel, P., and van Oudenaarden, A. (2007). Stochastic gene expression out-of-steady-state in the cyanobacterial circadian clock. *Nature* **450**, 1249–1252.
- Chen, Z., Odstrcil, E.A., Tu, B.P., and McKnight, S.L. (2007). Restriction of DNA replication to the reductive phase of the metabolic cycle protects genome integrity. *Science* **316**, 1916–1919.
- Clerico, E.M., Ditty, J.L., and Golden, S.S. (2007). Specialized techniques for site-directed mutagenesis in cyanobacteria. *Methods Mol. Biol.* **362**, 155–171.
- Dong, G., and Golden, S.S. (2008). How a cyanobacterium tells time. *Curr. Opin. Microbiol.* **11**, 541–546.
- Gregory, J.A., Becker, E.C., and Pogliano, K. (2008). *Bacillus subtilis* MinC destabilizes FtsZ-rings at new cell poles and contributes to the timing of cell division. *Genes Dev.* **22**, 3475–3488.
- Hayashi, F., Itoh, N., Uzumaki, T., Iwase, R., Tsuchiya, Y., Yamakawa, H., Morishita, M., Onai, K., Itoh, S., and Ishiura, M. (2004). Roles of two ATPase-motif-containing domains in cyanobacterial circadian clock protein KaiC. *J. Biol. Chem.* **279**, 52331–52337.
- Hayashi, F., Suzuki, H., Iwase, R., Uzumaki, T., Miyake, A., Shen, J.R., Imada, K., Furukawa, Y., Yonekura, K., Namba, K., et al. (2003). ATP-induced hexameric ring structure of the cyanobacterial circadian clock protein KaiC. *Genes Cells* **8**, 287–296.
- Hayashi, F., Iwase, R., Uzumaki, T., and Ishiura, M. (2006). Hexamerization by the N-terminal domain and intersubunit phosphorylation by the C-terminal domain of cyanobacterial circadian clock protein KaiC. *Biochem. Biophys. Res. Commun.* **348**, 864–872.
- Ishiura, M., Kutsuna, S., Aoki, S., Iwasaki, H., Andersson, C.R., Tanabe, A., Golden, S.S., Johnson, C.H., and Kondo, T. (1998). Expression of a gene cluster kaiABC as a circadian feedback process in cyanobacteria. *Science* **281**, 1519–1523.
- Ivleva, N.B., Bramlett, M.R., Lindahl, P.A., and Golden, S.S. (2005). LdpA: a component of the circadian clock senses redox state of the cell. *EMBO J.* **24**, 1202–1210.
- Ivleva, N.B., Gao, T., LiWang, A.C., and Golden, S.S. (2006). Quinone sensing by the circadian input kinase of the cyanobacterial circadian clock. *Proc. Natl. Acad. Sci. USA* **103**, 17468–17473.
- Iwasaki, H., Williams, S.B., Kitayama, Y., Ishiura, M., Golden, S.S., and Kondo, T. (2000). A kaiC-interacting sensory histidine kinase, SasA, necessary to sustain robust circadian oscillation in cyanobacteria. *Cell* **101**, 223–233.
- Iwasaki, H., Nishiwaki, T., Kitayama, Y., Nakajima, M., and Kondo, T. (2002). KaiA-stimulated KaiC phosphorylation in circadian timing loops in cyanobacteria. *Proc. Natl. Acad. Sci. USA* **99**, 15788–15793.
- Kawai, Y., Moriya, S., and Ogasawara, N. (2003). Identification of a protein, YneA, responsible for cell division suppression during the SOS response in *Bacillus subtilis*. *Mol. Microbiol.* **47**, 1113–1122.
- Kim, Y.I., Dong, G., Carruthers, C.W., Jr., Golden, S.S., and LiWang, A. (2008). The day/night switch in KaiC, a central oscillator component of the circadian clock of cyanobacteria. *Proc. Natl. Acad. Sci. USA* **105**, 12825–12830.
- Kitayama, Y., Iwasaki, H., Nishiwaki, T., and Kondo, T. (2003). KaiB functions as an attenuator of KaiC phosphorylation in the cyanobacterial circadian clock system. *EMBO J.* **22**, 2127–2134.
- Kitayama, Y., Nishiwaki, T., Terauchi, K., and Kondo, T. (2008). Dual KaiC-based oscillations constitute the circadian system of cyanobacteria. *Genes Dev.* **22**, 1513–1521.
- Kutsuna, S., Kondo, T., Ikegami, H., Uzumaki, T., Katayama, M., and Ishiura, M. (2007). The circadian clock-related gene pex regulates a negative cis element in the kaiA promoter region. *J. Bacteriol.* **189**, 7690–7696.
- Liu, Y., Tsinoremas, N.F., Johnson, C.H., Lebedeva, N.V., Golden, S.S., Ishiura, M., and Kondo, T. (1995). Circadian orchestration of gene expression in cyanobacteria. *Genes Dev.* **9**, 1469–1478.
- Lutkenhaus, J. (2007). Assembly dynamics of the bacterial MinCDE system and spatial regulation of the Z ring. *Annu. Rev. Biochem.* **76**, 539–562.
- Mackey, S.R., and Golden, S.S. (2007). Winding up the cyanobacterial circadian clock. *Trends Microbiol.* **15**, 381–388.
- Mackey, S.R., Ditty, J.L., Clerico, E.M., and Golden, S.S. (2007). Detection of rhythmic bioluminescence from luciferase reporters in cyanobacteria. *Methods Mol. Biol.* **362**, 115–129.
- Margolin, W. (2005). FtsZ and the division of prokaryotic cells and organelles. *Nat. Rev. Mol. Cell Biol.* **6**, 862–871.
- Matsuo, T., Yamaguchi, S., Mitsui, S., Emi, A., Shimoda, F., and Okamura, H. (2003). Control mechanism of the circadian clock for timing of cell division in vivo. *Science* **302**, 255–259.
- Mazouni, K., Domain, F., Cassier-Chauvat, C., and Chauvat, F. (2004). Molecular analysis of the key cytochemical components of cyanobacteria: FtsZ, ZipN and MinCDE. *Mol. Microbiol.* **52**, 1145–1158.
- Mihalcescu, I., Hsing, W., and Leibler, S. (2004). Resilient circadian oscillator revealed in individual cyanobacteria. *Nature* **430**, 81–85.
- Miyagishima, S.Y., Wolk, C.P., and Osteryoung, K.W. (2005). Identification of cyanobacterial cell division genes by comparative and mutational analyses. *Mol. Microbiol.* **56**, 126–143.
- Mori, T. (2009). Cell Division Cycles and Circadian Rhythms. In *Bacterial Circadian Programs*, J.L. Ditty, S.R. Mackey, and C.H. Johnson, eds. (New York: Springer), pp. 183–204.
- Mori, T., and Johnson, C.H. (2001). Independence of circadian timing from cell division in cyanobacteria. *J. Bacteriol.* **183**, 2439–2444.
- Mori, T., Binder, B., and Johnson, C.H. (1996). Circadian gating of cell division in cyanobacteria growing with average doubling times of less than 24 hours. *Proc. Natl. Acad. Sci. USA* **93**, 10183–10188.
- Nagoshi, E., Saini, C., Bauer, C., Laroche, T., Naef, F., and Schibler, U. (2004). Circadian gene expression in individual fibroblasts: Cell-autonomous and self-sustained oscillators pass time to daughter cells. *Cell* **119**, 693–705.
- Nakajima, M., Imai, K., Ito, H., Nishiwaki, T., Murayama, Y., Iwasaki, H., Oyama, T., and Kondo, T. (2005). Reconstitution of circadian oscillation of cyanobacterial KaiC phosphorylation in vitro. *Science* **308**, 414–415.
- Nishiwaki, T., Iwasaki, H., Ishiura, M., and Kondo, T. (2000). Nucleotide binding and autophosphorylation of the clock protein KaiC as a circadian timing process of cyanobacteria. *Proc. Natl. Acad. Sci. USA* **97**, 495–499.

- Nishiwaki, T., Satomi, Y., Nakajima, M., Lee, C., Kiyohara, R., Kageyama, H., Kitayama, Y., Temamoto, M., Yamaguchi, A., Hijikata, A., et al. (2004). Role of KaiC phosphorylation in the circadian clock system of *Synechococcus elongatus* PCC 7942. *Proc. Natl. Acad. Sci. USA* *101*, 13927–13932.
- Nishiwaki, T., Satomi, Y., Kitayama, Y., Terauchi, K., Kiyohara, R., Takao, T., and Kondo, T. (2007). A sequential program of dual phosphorylation of KaiC as a basis for circadian rhythm in cyanobacteria. *EMBO J.* *26*, 4029–4037.
- Rust, M.J., Markson, J.S., Lane, W.S., Fisher, D.S., and O'Shea, E.K. (2007). Ordered phosphorylation governs oscillation of a three-protein circadian clock. *Science* *318*, 809–812.
- Schmitz, O., Katayama, M., Williams, S.B., Kondo, T., and Golden, S.S. (2000). CikA, a bacteriophytochrome that resets the cyanobacterial circadian clock. *Science* *289*, 765–768.
- Smith, R.M., and Williams, S.B. (2006). Circadian rhythms in gene transcription imparted by chromosome compaction in the cyanobacterium *Synechococcus elongatus*. *Proc. Natl. Acad. Sci. USA* *103*, 8564–8569.
- Takai, N., Ikeuchi, S., Manabe, K., and Kutsuna, S. (2006a). Expression of the circadian clock-related gene *pex* in cyanobacteria increases in darkness and is required to delay the clock. *J. Biol. Rhythms* *21*, 235–244.
- Takai, N., Nakajima, M., Oyama, T., Kito, R., Sugita, C., Sugita, M., Kondo, T., and Iwasaki, H. (2006b). A KaiC-associating SasA-RpaA two-component regulatory system as a major circadian timing mediator in cyanobacteria. *Proc. Natl. Acad. Sci. USA* *103*, 12109–12114.
- Terauchi, K., Kitayama, Y., Nishiwaki, T., Miwa, K., Murayama, Y., Oyama, T., and Kondo, T. (2007). ATPase activity of KaiC determines the basic timing for circadian clock of cyanobacteria. *Proc. Natl. Acad. Sci. USA* *104*, 16377–16381.
- Tomita, J., Nakajima, M., Kondo, T., and Iwasaki, H. (2005). No transcription-translation feedback in circadian rhythm of KaiC phosphorylation. *Science* *307*, 251–254.
- Wang, J. (2004). Nucleotide-dependent domain motions within rings of the RecA/AAA(+) superfamily. *J. Struct. Biol.* *148*, 259–267.
- Wear, R.B., Lee, A.H., Chien, A.C., Haeusser, D.P., Hill, N.S., and Levin, P.A. (2007). A metabolic sensor governing cell size in bacteria. *Cell* *130*, 335–347.
- Williams, S.B., Vakonakis, I., Golden, S.S., and LiWang, A.C. (2002). Structure and function from the circadian clock protein KaiA of *Synechococcus elongatus*: a potential clock input mechanism. *Proc. Natl. Acad. Sci. USA* *99*, 15357–15362.
- Xu, Y., Mori, T., Pattanayek, R., Pattanayek, S., Egli, M., and Johnson, C.H. (2004). Identification of key phosphorylation sites in the circadian clock protein KaiC by crystallographic and mutagenetic analyses. *Proc. Natl. Acad. Sci. USA* *101*, 13933–13938.
- Ye, J., Osborne, A.R., Groll, M., and Rapoport, T.A. (2004). RecA-like motor ATPases—lessons from structures. *Biochim. Biophys. Acta* *1659*, 1–18.
- Zhang, X., Dong, G., and Golden, S.S. (2006). The pseudo-receiver domain of CikA regulates the cyanobacterial circadian input pathway. *Mol. Microbiol.* *60*, 658–668.